Secondary flows occurring in a whirlpool separator – A study of phenomena – observation, simulation and measurements

Marek Jakubowski[*]

Koszalin University of Technology, Faculty of Mechanical Engineering, Department of Food Industry Processes and Facilities, Raclawicka 15-17,75-620 Koszalin, Poland

The whirlpool separator, used for hot trub separation, is prevalent in the brewing industry. It is a kind of a hydrocyclone inside of which a tea leaf effect occurs, which is sediment accumulation into a cone shape at the central part of the tank's bottom. This manner of sediment accumulation is caused by the secondary flow occurring in the so-called Ekman boundary layer. This article is a summary of the research, which has been conducted for many years and involved observation, simulation and experimental research on the recognition and formation of the secondary flow accumulating the sediment cone. Secondary flows occurring in a whirlpool were identified through CFD simulation and PIV experiments, and are presented in this paper. Based on their location and direction, an attempt to determine their impact on the separation process taking place in the whirlpool has been made. The secondary flow identification methods proposed in this paper can be successfully applied in other solutions, e. g. structural ones, which involve rotational-flow-based separation.

Keywords: whirlpool, CFD, PIV

1. INTRODUCTION

Brewing techniques and technology have been evolving over the centuries, and this has led to the development of processing standards. One such standard is to use the so-called whirlpool (Fig. 1a) to separate hot trub from the beer wort.

Cycling vat (as a type of a hydrocyclone) is a prevalent as well as an effective solution. It has a form of a closed cylindrical tank. It is filled through an inlet placed tangentially in its wall. As a result, the primary flow is formed, which causes the clarified wort to rotate. Sedimentation of particles of the separated hot trub happens gravitationally and is amplified by the mixture rotational motion.

A secondary flow forms itself in the so-called Ekman boundary layer inside the separator (Denk and Dürholt, 1991). Due to sedimentation, along with an aggregate of secondary flows caused by rotational flow, the separated hot trub forms a cone in the centre of the tank. This way of forming and accumulation of solid phase was originally described by Albert Einstein and called the "Tea leaf effect" or "Tea leaf paradox" (Einstein, 1926).

Apparatuses implementing the phenomenon of forming the sediment into a cone in order to separate the solid phase from the mixture are also used in other fields of food processing, chemical engineering

---

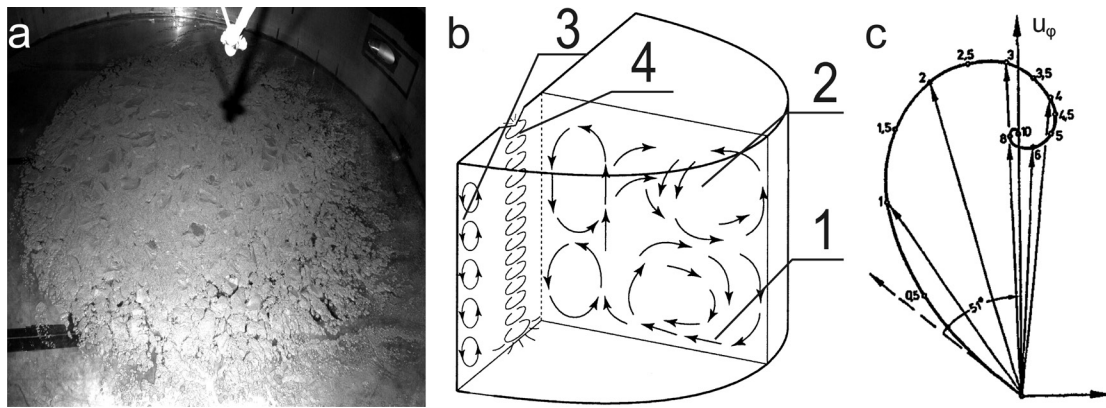* Corresponding author, e-mail: marek.jakubowski@tu koszalin.pl

Fig. 1 Whirlpool: a) a general view of the interior after hot trub separation; b) a diagram of secondary flows:
1 –the flow accumulating the sediment cone, 2 – the central whirl, 3 – Taylor-Görtler vortices, 4 – vortex orbiting around the fluid's rotation axis; c) particle trajectory at the tank's bottom – Ekman spiral

and medicine (e.g. for separation of red blood cells from blood plasma (Arifin et al., 2007)) and also in wastewater treatment (e.g. in Geiger, 1937).

The aim of this work was to identify secondary flows in terms of their location and impact on the sediment accumulation effect inside the whirlpool separator. An analysis allowed to verify opinions found in literature regarding the system of secondary flows present in centrifugal separators.

1.1. Flows inside the whirlpool

Apart from the primary flow (being a consequence to the specific manner of filling the tank) there are also secondary flows. They constitute a flow system, which thus far remains virtually unexplored. This system is in general unsteady. Secondary flows have a strong impact on the separation process and the position of sediment particles. The knowledge base in the form of e.g. diagrams depicting the position of secondary flows is for visual purposes only (e.g. Fig. 1b) and is derived from observation of their impact.

During the swirling of the fluid and dispersed phase mixture the flow becomes unsteady due to central, near-wall Taylor-Görtler vortices and a vortex tube revolving around the centre of the primary flow paraboloid of revolution free surface. From the technological and processing standpoint, the most impactful secondary flow is the rotational flow near the separator bottom in the Ekman boundary layer (Denk and Dürholt, 1991). This flow causes the separated sediment to form a cone.

1.2. The flow accumulating the sediment cone and the Ekman spiral

The formation of the secondary flow accumulating the sediment just above the surface to the whirlpool bottom is connected with the so-called rotating fluid's boundary layer effect. At the core of this phenomenon lay frictional forces present in the layer of fluid being in contact with the tank bottom. Further away from that area the flow motion is not retarded and is oriented outward (in accordance with the rotational motion centrifugal force). It results in pressure increase in outer areas (near the shell-to-bottom joint). The consequence is that the fluid travels to the tank inner areas due to pressure drop at the central part of the tank bottom. And therefore the secondary flow occurrence is a result of pressure unsteadiness in the fluid boundary layer at the tank bottom and is dependent upon hydrostatic pressure (varying along the radius). Inside the whirlpool the prevailing flow direction is around the tank circumference, as a result of the filling manner. In the boundary layer at the tank bottom the value of circumferential flow velocity is much reduced due to breaking condition satisfaction. The aforementioned secondary flow is oriented inward in accordance with the radial component. The result of those flow directions colliding with each other is that near the

boundary layer the hot trub will travel along spiral trajectories towards the tank's bottom's center. This is what we call the Ekman spiral (Fig. 1c based on Dürholt (1988)). This phenomenon is widely known in the meteorology theory and is described as bending of streamlines above the spinning Earth surface.

2. MATERIAL AND METHODS

Presented below are methods and setups which were used in the visualisation of the sediment cone formation, CFD analysis and PIV measurements.

2.1. Employing substitute sediment

A test bench with a laboratory whirlpool tank (Fig. 2, on the right), made of methyl polymetacrylate (PMMA) was used for the visualisation of sediment cone formation stages. The tank diameter was $D = 0.64$ m and the nominal filling height was $H = 0.64$ m. In order to make the research on the impact of the inlet situation on the cone formation phenomenon possible the tank had a set of nine inlets, six of which were situated higher than we typically see in industrial apparatuses. The spectrum of this paper covers only the filling manner that used the inlet closest to the bottom.
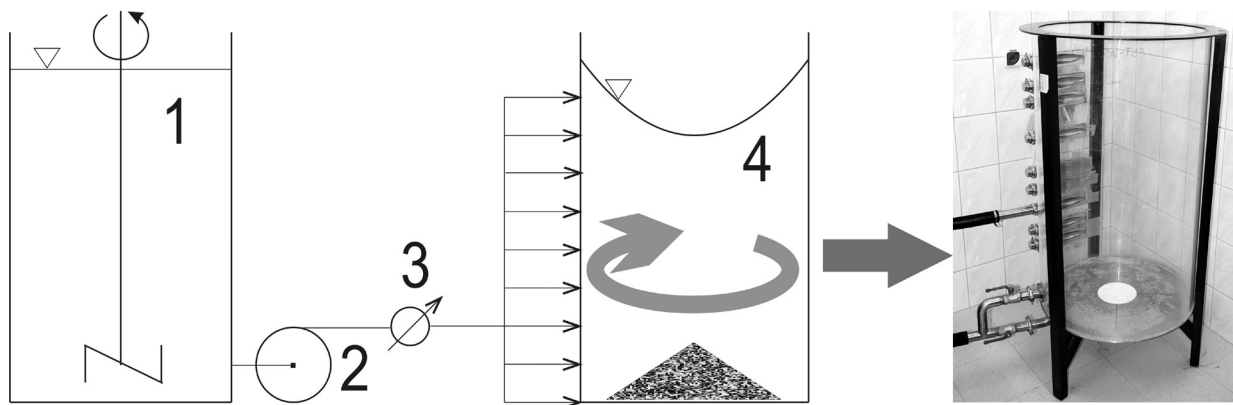

Fig. 2. The test stand a) diagram: 1) the container for preparing the mixture, 2) pump type FAM GA-12, 3) flowmeter PM390, 4) laboratory whirlpool vat (view of inlets are presented on the right side)

The setup also provided a preliminary tank (equipped with a turbine impeller) used for preparing the model mixture. The setup had a flowmeter and an optional pump connected with pipelines. Figure 2 presents a diagram of the test stand.

Polymeric particles (PA) were used as the substitute sediment. The filling was performed at a constant rate of $u_i = 1.7$ m·s^{-1}, with $H/D = 1$. Also, the inlet closest to the tank's bottom was used. The sediment concentration was 1%. Table 1 compares sizes of typical process parameters of whirlpool tanks used in the research.

Table 1. Structural and process parameters of test tanks used in the research

parameter	visualisation tank	CFD tank	PIV tank
D	0.64	0.196	0.196
H	0.64	0.196	0.196
H/D ratio	1	1	1
h_i	0.08	0.0127	0.0127
ϕ_i	0.05	0.007	0.007
u_i	1.7	1.2	1.2

2.2. CFD model

The simulation was performed using a commercial CFD code implemented in the ANSYS CFX 12.1 environment. The simulation employed the control volume – finite element method (CV-FEM). It allows to solve numerically a set of balance equations which specify the motion of a liquid (Duarte and Cristianini, 2012). Obviously, it is necessary to declare model boundary conditions as well as the simulation initial conditions. A geometrical model of the separator tank was designed, with an area declared as an inlet situated at the height corresponding with the inlet of the PIV tank, described later in this paper. Using the Mechanical APDL 12.1 software program model, a geometrical space was generated and its discretisation was performed (by meshing the cylindrical space – Fig. 3a) using structural FEM mesh (Fig. 3b) with a three-dimensional type of mesh element appropriate for the flow simulation.
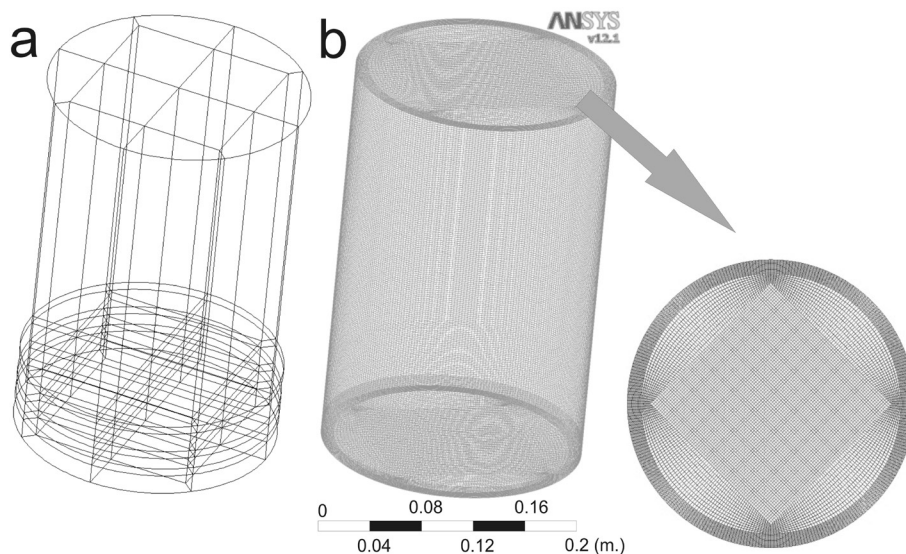

Fig. 3. The CFD model: a) model geometry with marked division section, b) the FEM grid

The generated mesh consisted of approximately 1,800,000 elements, which in the area of the tank wall and bottom were packed particularly densely in order to ensure the correctness of the analysis of the flow phenomena occurring close to the boundary layer near the tank wall and bottom. The model depicted in Fig. 3b was designed to be versatile and applicable to simulation of filling with inlets situated at different heights as well as multi-sided filling. The filling rate $u_i = 1.2$ m·s^{-1} was set as the initial condition of the simulation. It is whirlpool nominal filling rate, advised for the separation process in industrial operation (Kunze, 2014). This value was determined on the basis of the flow intensity in the experimental PIV research, presented below. The case was modeled as turbulent using an SST model (*Škerlavaj* et al., 2014) with coefficients modified on the basis of adaptation work based on the analysis of similar phenomena occurring in the rotational flow. The filling process was simulated as a flow with a free surface. This type of simulation is based on volume of fluid (VOF). At the inlet, there was inflow of two phases, the fraction of which was fluid=1 and air=0, as it was necessary to achieve the free surface. Air did not mix with the fluid, therefore the system had been previously specified as pseudo single-phase, even thougt CFD solver actually has to solve a system typical of a two-phase flow.

As for the inlet, the model had boundary conditions declared as delimited surfaces on the cylinder's wall. The cylinder's upper base's surface had a condition of type open, in accordance with the assumption that the tank was initially completely filled with air at atmospheric pressure. As the filling progressed, the air was pushed from the tank by the inflowing fluid. The rest of the boundary conditions were declared at the tank's wall. For more on the mathematical model, its boundary and initial conditions, choosing the simulation time step and testing the CFD model refer to Jakubowski et al. (2014) and Jakubowski et al. (2015).

Because of the concentration level of the wort hot trub (under 1%) the flow was modelled, for simplicity, as single-phased. The fluid physical properties (as a material) corresponded to beer wort in a standard state. This simplification had to be declared in the model, in order to make sure that later experimental verification using PIV research would be possible to conduct under matching conditions.

2.3. The PIV test bench

The experimental research employed particle image velocimetry (PIV). It is a flow analysis method, which uses seeding particles. The particles are of a very small size (varying from a few to a few dozen micrometers) and they are introduced into the analysed medium. For the analysis of the fluid flow inside a whirlpool 20 μm polyamide (PA) particles were used. The seeding particles follow the flow and do not cause any interference in the analysed medium. During the measurement they are illuminated with a sheet of laser light, which is diffused on their surface. The shift of the seeding particles is captured with a camera (or cameras) as double frames (two expositions in one image separated by a short time interval) which later on serve as the base for the cross-correlation. Using the shift values the flow's velocity vector can be determined.

The PIV method is particularly advantageous in the fields of flow velocity into which, for some reasons, we cannot introduce a measuring sensor – just like in the whirlpool case. When it comes to such a specific flow of fluid, an introduction of a measuring sensor into a tank would have generated disturbances of the flow, therefore the sensor would have measured a value encumbered with error resulting from the presence of the sensor itself. For this reason the most suitable method in the case of flows in a whirlpool was an optical one.

The test bench was built in R&D Philadelphia Mixing Solutions, Palmyra, PA. Figure 4a presents a sketch of the test bench with its key elements marked. The measurements employed a FlowSense 2M PIV camera and a NewWave Solo 120 TX double-pulsed YAG laser with a water-cooled controller. Synchronisation was done using System Hub DantecDynamics. A 6-liter (1.58-US-gallon) test tank (Fig. 4b) was designed and built. The tank was made of PMMA. The choice of the material was a compromise between durability and transparency – this material is of scarce hardness, which makes it scratch-prone. Deep scratches cause image distortions, in most cases rendering them useless for further processing.
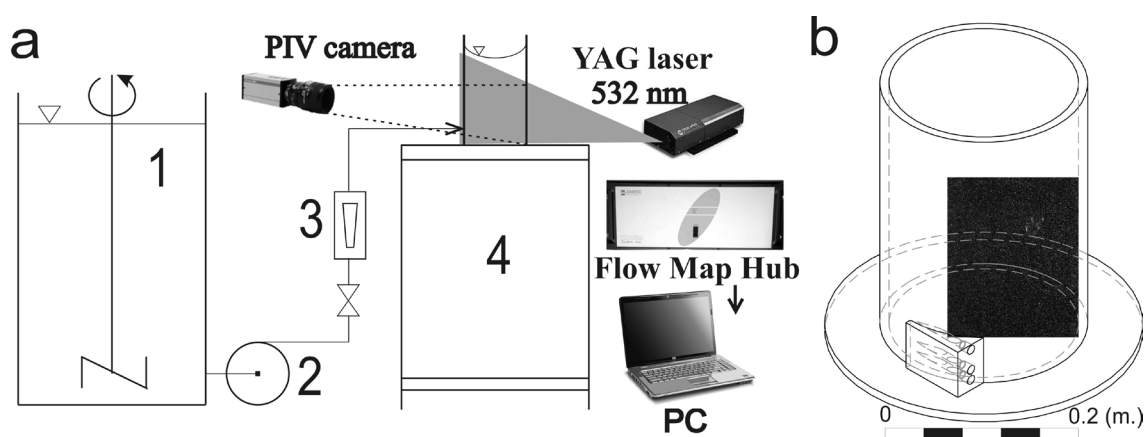

Fig. 4. The test bench: a) the sketch of the test tank with a light-enter area marked, b) the diagram: 1) the tank for preparing the mixture of water and seeding particles, 2) the VANTON FLEX-I-LINER pump, 3) a rotameter, 4) the workbench for PIV measurements

The tank was filled using the inlet closest to the bottom. The filling with water and seeding particles was conducted at the rate of 0.8 gpm (which after conversion is equal to $u_i = 1.2$ m·s^{-1}). The water we used contained an additive of sugar increasing its density. This was done in order to match the mixture to the physical properties of wort at 25°C.

Due to the specificity of this research (flow measurement for the radial component) it was necessary to use a sheet of laser light oriented vertically. To avoid image distortions a compensational tank was used on the surface of tank cylindrical wall, which reduced image deformation at the tank wall. The tank was placed inside a bigger, cuboidal tank filled with a test fluid, appropriate for the conducted PIV research.

For the horizontal orientation of the light sheet about 30 measurements were performed. Each measurement comprised two attempts, for which different time intervals between laser pulses were declared. The delay of the second pulse for this variant of exposition was declared between 1000 µs and 2800 µs. This was connected with the lack of ability to seamlessly alter the time interval between pulses. It is important in the case of a transient flow, occurring in the whirlpool. Such a time interval setting allowed us to measure the distance a particle travelled within the interrogation cell, which also guaranteed that we would get data appropriate for the analysis at the beginning and at the end of spinning. The whole PIV research plan covered over 250 measurements, yet the principle was to perform measurements only for the horizontal orientation of the light sheet. So, any further considerations were constrained to typical vertical exposure.

The obtained images of seeding particle shift were double frames exposed by two laser impulses. The time interval between them was varying. At the beginning of the spinning it was 1000 µs, and it gradually increased with every consecutive stage. The images were captured at 1 Hz frequency. For further analysis we chose images representing a full second of spinning. The time of the measurement was equal to the time of spinning. After saving them in databases they were initially processed. The applied technique was map image processing, the aim of which was to eliminate elements shared across all images. Thereby, light reflections at the tank wall were eliminated and the flare at the fluid-wall boundary was reduced. The material prepared in such a manner was then a subject to cross correlation analysis with the interrogation area size set to 64×64 pixels. Due to unsteadiness of the flow it was possible to analyse only one double frame at a time. The resulting maps of whirlpool flow vector fields depict only locally changing velocity values of the illuminated section.

3. RESULTS AND DISCUSSION

Below are presented the results of observation, simulation and experimental research on the formation and recognition of the secondary flow forming the sediment cone. The presented data are a part of an entity and, by the author's intentions, they are to be regarded as a study of the secondary flow identification, which can be a starting point for seeking new solutions for the separator structure modification and separation technology. Therefore, some of the characteristic states of flow occurring inside a whirlpool have been presented in order to depict secondary flows. Some of the values were treated as of minor significance, e.g. dimensionless numbers which specify the flow, because they strongly depend on the filling velocity value and the investigated area of occurrence. For example, German authors claim that the critical value of the Reynolds number for the accumulating flow present in the Ekman layer is equal to $Re = 0.7$ (Dürholt, 1988). This value, except for the numerical expression, does not provide any information about the characteristics of the flow in this layer.

3.1. Cone formation visualisation

Figure 5 presents photographs depicting characteristic geometrical stages of sediment cone formation. Based on many observations and repeated filming of spinning it was determined that the cone formation manner is very specific, which allows to identify its characteristic stages. During swirling, sediment particles are initially clustered and they begin to form a torus-like circle (Fig. 5a). Then, the torus is fully formed (Fig. 5b), and we can observe a constant reduction of its internal diameter length, which leads to closing and forming a rudiment of a cone (Fig. 5c). At this stage (for some of the filling manner variants)

one could observe on the cone surface a temporary vortex tube (or two), which would cause the sediment to travel upward for a very short period. Afterward, the cone would spin with the fluid (Fig. 5d), and after it formed into stationary cone (Fig. 5e), but particles at the surface would spirally travel toward the tank centre. With time the liquid would stop spinning and the substitute sediment cone would form its final geometric shape (Fig. 5f).
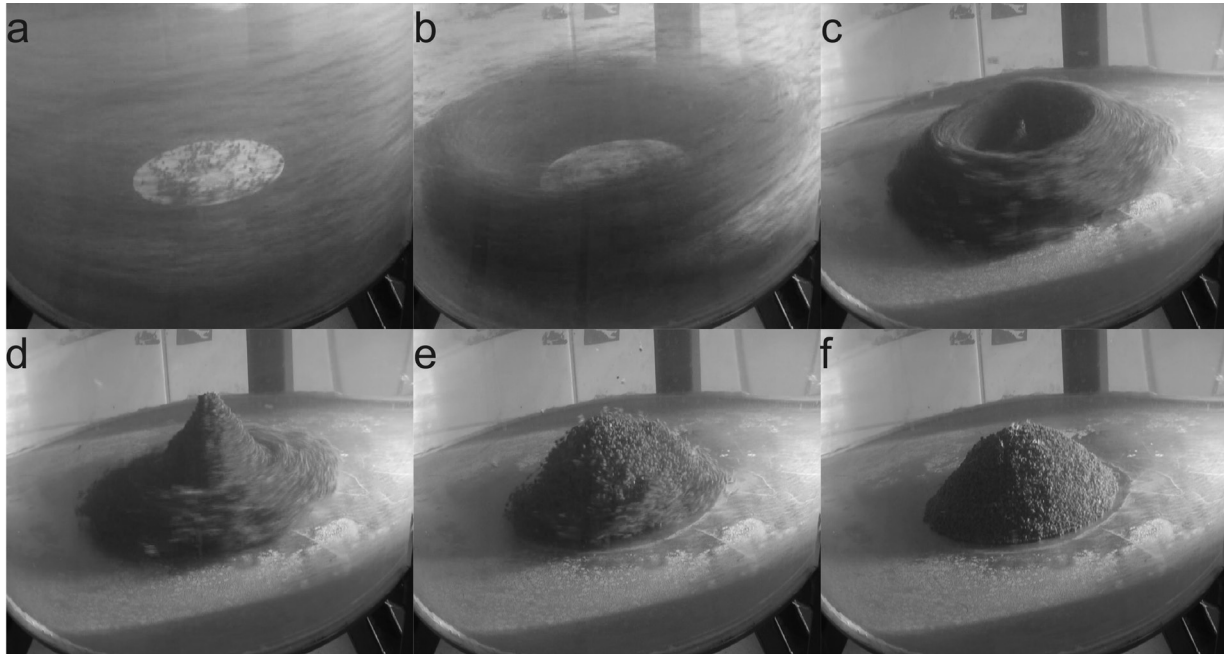

Fig. 5. The stages of substitute sediment cone formation: a) the particles flowing in the tank's outer regions ($t = 40$ s), b) the beginning of torus formation ($t = 100$ s), c) the torus has closed ($t = 150$ s), d) the spinning cone with a form encouraging vortex tube occurrence ($t = 220$ s), e) the spinning sediment cone ($t = 430$ s), f) the fully formed sediment cone – the end of spinning ($t = 550$ s).

Filming the spinning allowed to determine the timing of substitute cone formation stages. This made it possible to learn about the impact of particular modifications of the separation as a technological operation conduct on the formation and development the cone-accumulating flow. Thus far, the timing of cone formation characteristic stages was compared with its relation to the height of filling, filling rate, height of the poured fluid, inlet's shape, tank bottom's tilt angle, and the bottom's shape (as a sediment plate or a cone-shape bottom).

3.2. The results of the simulation analyses

After a series of simulation computations the obtained output files were post-processed. As for the analysis, the flow close to the bottom was the interesting thing. Also an attempt to identify the near-wall vortices was made. To do so, vector maps of velocity field with zeroed velocity vector's angular component – for the period of fluid's rotation set as dominant – were generated. To achieve that, expressions based on the vector's components were designed using the CFX language, and then the resultant was computed with the angular component set to zero. As a result, maps of velocity fields (in the form of isolines) of fluid motion paths were generated for both the radial and the height components. This allowed us to obtain images of secondary flows, the maximum velocity value which was ten times smaller than the average velocity value of a rotating fluid. Figure 6 presents maps of secondary flow's velocity field occurring at the bottom of the whirlpool for the horizontally (Fig. 6a) and vertically (Figs. 6b and 6c) oriented sheets of light.

Figure 6 presents streamlines obtained in the layer typical of the accumulating flow occurrence. For all the velocity vector components with a dominant value of the circumferential component velocity set the

streamlines resemble the earlier described Ekman spiral. Figure 6b presents a vector map of velocity field with the velocity vector's circumferential component set to zero. This allows to plot the radial and longitudinal components. Due to substantial differences in velocity values between the primary flow and secondary flows, obtaining images of them is only possible for this type of exposition. There is a velocity-wise dominant flow present at the tank bottom. Its direction is from the shell-to-bottom joint to the bottom centre. This is the flow causing sediment particles to travel toward the separator centre. The flow shape analysis revealed it was much more stretched along the tank bottom than the literature suggests (e.g. Fig. b). This distinctive shape was also present in the 2D CFD model with swirl first approximation, presented in Jakubowski and Diakun (2007).
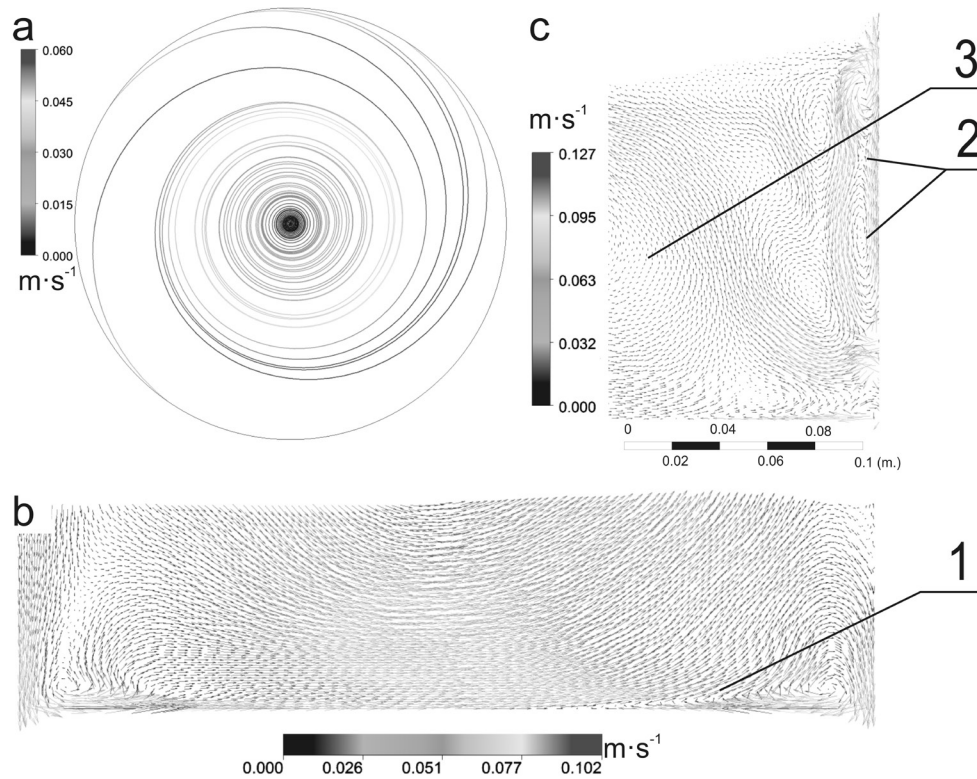

Fig. 6. Maps of secondary flows' vector field in a whirlpool model for: a) accumulating flow – horizontal exposition $t = 45$ s, b) accumulating flow – vertical exposition $t = 45$ s, c) near-wall flow – vertical exposition $t = 45$ s (where: 1-accumulating flow, 2-the Taylor-Görtler vortices, 3-the central vortex)

Another thing was to determine the occurrence and situation of the central flow. Fig. 6b presents a map on which it is visible above the accumulating flow. It has a considerable size and a circular cross section. It occurs in the tank central area and it is distinguishable only during a selected time period. Yet, it does not change its position and it impacts a significant amount of the fluid volume. Its shape diverges from what is present in the literature. On the other hand, its velocity values are approximately ten times smaller when compared to the accumulating flow. The central and accumulating flows are intertwined. The former constitutes an extension of the latter toward the tank upper area. It also causes the torus formation (as presented in the section about visualisation and in Figs. 5b and 5c).

The last stage of simulation data analysis identifies the near-wall flows (the Taylor-Görtler vortices). Figure 6c presents cross sections of the area close to the tank wall. The occurrence of the Taylor-Görtler vortices is a consequence to the flow interaction with the whirlpool wall. Those flows appear as a series of vortex pairs, and their impact is local and changes over time. As presented in Jakubowski (2011) they appear early in the filling stage and with time vortices begin to travel along the tank wall to eventually fade away.

3.3. The PIV measurement results

The in-whirlpool-spin fluid PIV measurement results were a reference point for the CFD model simulation data validation. Figure 7 presents sample images of secondary flows, including maps of vector fields where we can identify spiral lines (Fig. 7a) and the area of the accumulating flow (Fig. 7b). Just like the CFD analysis revealed, vertical exposure renders the accumulating flow's shape as flattened. This flow is also perfectly visible in Figs. 7b and 7c. It also shows its tendency to evolve, which means that the flow maximum velocity values travel toward the tank centre.

Figure 7b is the flow state, a part of which is made up of the near-wall flows (the Taylor-Görtler vortices). They appear as vortex pairs and have a travelling pattern, which confirms the results of the simulation analyses presented by Diakun and Jakubowski (2010). The vortex pairs begin to arise near the shell-to-bottom joint and travel toward the spinning fluid free surface. Their velocity values are over ten times smaller than those for the cone-accumulating flow. Taylor-Görtler vortices are transient, so they should be regarded as a part of the flow unsteadiness in the boundary layer near the tank wall.

Figure 7c presents the central vortex forming in the whirlpool flow. It has the same direction as the accumulating flow, which was earlier discussed in the CFD analysis section. This flow has also significantly smaller velocity values than the accumulating flow. The experimental verification confirms its direct connection with the accumulating flow, just like the CFD analyses did.

Comparing velocity field maps obtained from the PIV research to the maps resulting from the CFD simulation it should be noticed that in spite of some minor discrepancies in both cases distinguishable secondary flows are present. The flows taking place at the tank wall are transient, so their identification timing may be distinct from what is present in the results of the simulation.
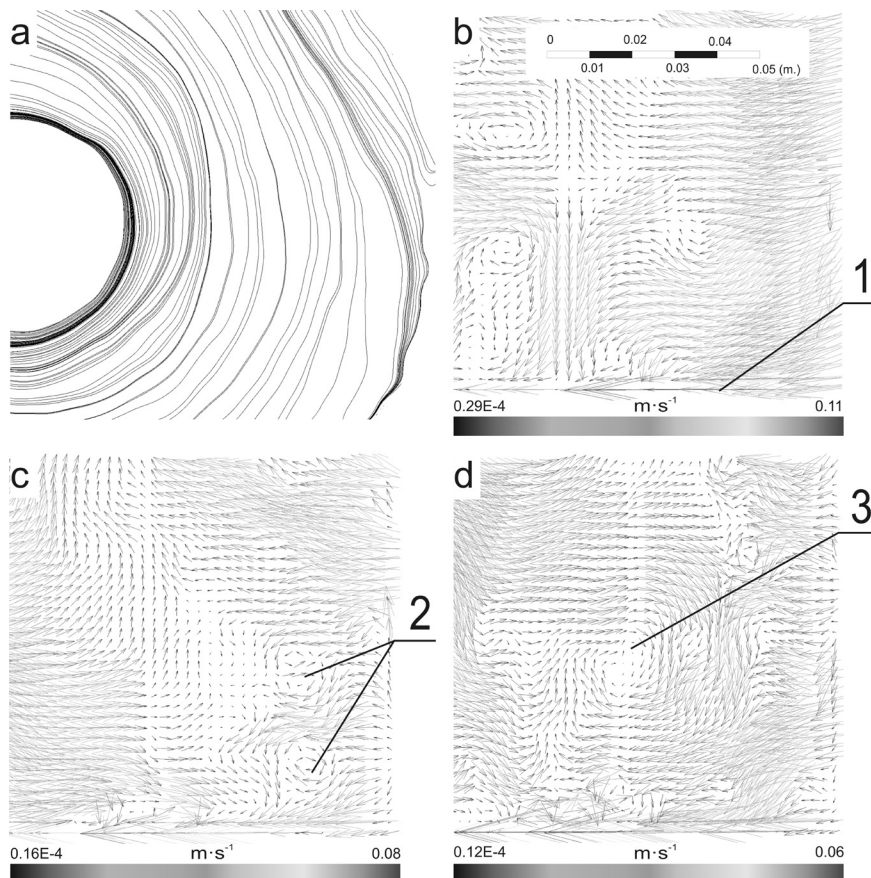

Fig. 7. Maps of secondary flows' velocity in a PIV whirlpool model at: a) *t* = 36s (horizontal exposition resulting in streamlines) b) *t* = 36 s, c) *t* = 85 s, d) *t* = 98 s (where: 1-accumulating flow, 2-the Taylor-Görtler vortices, 3-the central vortex)

The same principle applies to the comparison of the central flow. The only constantly present flow is the one accumulating the sediment cone (depicted in Fig. 7d). It should be taken into account that a simulation (even prepared and conducted in the most careful manner) is a mere approximation of the real world. This is especially true in the case of an unsteady flow with locally occurring secondary flows. This is the type of flow we dealt with while analysing whirlpool flows. Still, the results of the PIV measurements alone provide data allowing to conduct research on optimisation of this type of separator structures. Such results can be scaled up. To read more about this topic see Diakun and Jakubowski (2013).

3.4 Scale-up

An analysis of flows in whirlpools of identical or different dimensional proportions and diverse initial parameters, characteristic of flow and separation, requires scaling. Speaking of the presented results of the CFD simulation and the PIV measurement analysis, the researched object had the same dimensions and initial conditions as far as flow parameters were concerned. However, the whirlpool used for visualisation had greater dimensions, and the initial conditions differed from the ones declared in the analysis.

When it comes to scaling, there are multiple approaches connected with dimensional similarity of whirlpools. The fundamental parameter is the *H:D* ratio, that is the relation between the liquid column and the tank's diameter after it has been filled. In the cases of whirlpools presented in the paper, that ratio was equal to 1. The same is true for the situation and area of the inlet. And so the structural and dimensional similarity on its own does not provide means for full scaling of this type of separator. A more general approach should define similarity between whirlpools as a function of structural and process variables, and dimensionless criteria numbers specifying the flow system.

Relations between dimension proportions allow to determine the similarity of two whirlpool separators of different capacity, provided that the proportion between dimensions is maintained. As far as similarity of flows is considered, the key parameter is the dominant (angular) velocity component. The function, in its general form, is identical to what other authors presented (Dürholt, 1988):

$$u_\varphi = f\left(r, z, u_i, d_i, h_i, D, H, g, \nu\right) \tag{1}$$

which after transformation is expressed as:

$$\frac{u_\varphi}{u_i} = F\left(\frac{r}{R}, \frac{z}{Z}, \frac{d_i}{D}, \frac{h_i}{H}, \frac{H}{D}, Fr, Re\right) \tag{2}$$

Dimensionless criteria numbers (Froude and Reynolds) for the formula are:

$$Fr = \frac{u_i^2}{g \cdot d_i}, \tag{3}$$

and:

$$Re = \frac{u_i \cdot d_i}{\nu} \tag{4}$$

Reynolds number modified specifically for the whirlpool (Denk and Dürholt, 1991) is:

$$Re_{whirl} = \frac{R^2}{\nu \cdot t} \tag{5}$$

Since it is possible to determine the scale for the time of swirling in the model and in the whirlpool of greater dimensions, in the form of:

$$\frac{t_{whirl}}{t_{model}} = \frac{\nu_{model}}{\nu_{whirl}} \cdot \left(\frac{R_{whirl}}{R_{model}}\right)^2. \tag{6}$$

Another approach was an analysis based on a comparison of quotients of interactions (e.g. of forces) occurring in the flow inside the whirlpool. An analysis was carried out, which allowed to formulate a set of criteria numbers. A modified Reynolds number for the secondary flow was proposed:

$$Re = \frac{u \cdot D}{v} \cdot \frac{K_{hb}}{K_{ub}} \tag{7}$$

where $K_{hb} = \dfrac{h_b}{D}$ and $K_{ub} = \dfrac{u_b}{u}$.

Strouhal number was introduced as the dimensionless number characterising the unsteady flow:

$$St = \frac{D}{u \cdot t}. \tag{8}$$

and also our own number, which characterises the ratio of inertial force to viscous dissipation force for the dissipation of the primary flow:

$$K_{diss} = \frac{\dfrac{u}{t} \cdot D^2 \cdot H \cdot \rho}{u \cdot \mu \cdot H} = \frac{D^2}{v \cdot t} \tag{9}$$

In the process of transformation, criteria numbers for swirling time and parameters of the secondary flow forming the sediment cone were identified. Two functions of criteria numbers were proposed. They allow to determine the swirling time and they also describe the parameters of the secondary flow accumulating the sediment cone.

The derived dependencies may turn out to be helpful in the process of designing whirlpool tanks, as well as in scaling the flow occurring inside them. For more information please refer to (Diakun and Jakubowski, 2013).

4. THE PROSPECTS

In terms of learning about the nature of whirlpool flows there is PIV research being conducted on the impact of the introduction of a reduced baffle to the separator tank internal structure. As stated in the assumptions of the P.407021 patent application, a specifically shaped structural element attached to the tank bottom will allow to direct the primary flow in an advantageous manner toward the centre of the tank bottom, thereby allowing better utilisation of the rotational motion that would enhance the separation process (Sterczyńska et al, 2014).

5. CONCLUSIONS

The nature of the cycling vat secondary flows is very complex. Even a rough analysis suggests what their advantages and disadvantages on the whirlpool effect are. Apart from the clearly advantageous impact of the accumulating flow, which constitutes the essence of the whirlpool effect, also other secondary flow have been recognised.

When it comes to near-wall vortices, based on the CFD modelling and PIV measurement results, it has been determined that their impact is mediocre. These flows can carry hot trub from the separator wall to its central area, yet their upward travelling pattern may act against trub sedimentation. The last argument is the fact that near-wall vortices appear only during a narrow time period, mostly while the final-stage-of-filling flow is stabilising.

The central flow is in general also very mediocre. It may encourage the sediment travelling toward the area of the accumulating flow impact. But it is characterised by steadiness, which means it may change

its position or even – temporarily – its direction. Therefore, when it happens above the forming sediment – after the torus has closed – it may cause the cone upper regions to diffuse.

Similar flow systems are also present in other types of separators having a cylindrical separation tank. Therefore, applying our considerations and suggested solutions onto other constructions, which take advantage of the rotational-motion-based separation, appears feasible.

SYMBOLS

D	tank diameter, m
d	inlet diameter, m
Fr	Froude number
g	gravitational acceleration, $m \cdot s^{-2}$
H	filling height, m
h	inlet height, m
K	dimensionless number (in general),
R	whirlpool radius, m
Re	Reynolds number
St	Strouhal number
t	time, s
u	velocity, $m \cdot s^{-1}$

Greek symbols

μ	dynamic viscosity, $Pa \cdot s$
v	kinematic viscosity, $m^2 \cdot s^{-1}$
ρ	density, $kg \cdot m^{-3}$
ϕ	diameter, m

Subscripts

diss	dissipation
i	inlet, filling
m	model (smaller whirlpool)
w	whirlpool, bigger vessel

REFERENCES

Arifin D.R, Yeo L.Y., Friend J.R., 2007. Microfluidic blood plasma separation via bulk electrohydrodynamic flows. *Biomicrofluidics*, 1, 014103. DOI: 10.1063/1.2409629.

Denk V., Dürholt A., 1991. Experimental investigations of the unsteady rotating flow field in a cylindrical vessel. *Exp. Fluids*, 12, 97-105. DOI: 10.1007/BF00226572.

Diakun J., Jakubowski M., 2010. Analysis of the secondary flow velocities forming a settling cone in a whirlpool vat. *Chem. Process Eng.*, 31, 477–488.

Diakun J., Jakubowski M., 2013. Dimensionless numbers of structural and process similitude of a whirlpool hot trub separator. *J. Food Process Eng.*, 36, 748–752. DOI: 10.1111/jfpe.12043.

Duarte A.P.E., Cristianini M., 2012. Using Computational Fluid Dynamics (CFD) for evaluation of fluid flow through a gate valve. *Int. J. Food Eng.*, 8. DOI: 10.1515/1556-3758.2207.

Dürholt A., 1988. Experimental investigation of the unsteady rotational flow in the settling vessel "whirlpool". *Fortschr.-Ber. VDI* 14(38), 24–28. VDI-Verlag Düsseldorf (in German).

Einstein A., 1926. The cause of the formation of meanders in the courses of rivers and of the so-called Baer's law. *Naturwissenschaft*, 14, 2, 223–224 (in German).

Geiger H., 1937. *Sand Trap*. US Patent 2088294.

Kunze W. *Technology brewing and malting*. 2014, VLB, Berlin, 356–360.

Jakubowski M., Diakun J., 2007. Simulation investigations of the effects of whirlpool dimensional ratios on the state of secondary whirls. *J. Food Eng.*, 1, 107–110. DOI: 10.1016/j.jfoodeng.2006.12.025.

Jakubowski M., 2011. Three-dimensional model of fluid flow in the whirlpool, *Technol. Progress Food Process.*, 1, 24-28 (in Polish).

Jakubowski M., Sterczyńska M., Matysko R., Poreda A., 2014. Simulation and experimental research on the flow inside a whirlpool separator. *J. Food Eng.*, 133, 9-15. DOI: 10.1016/j.jfoodeng.2014.02.011.

Jakubowski M., Wyczalkowski W., Poreda A., 2015. Flow in a symmetrically filled whirlpool: CFD modelling and experimental study based on Particle Image Velocimetry (PIV). *J. Food Eng.*, 145, 64-72. DOI: 10.1016/j.jfoodeng.2014.08.009.

Sterczyńska M., Jakubowski M., Tuszyński T., 2014. *The swirling vat used particularly in brewing process and method of filling it*. National Patent Application; P.407021 (in Polish).

Škerlavaj A., Škerget L., Ravnik J., Lipej A., 2014. Predicting free-surface vortices with single-phase simulations. *Eng. Appl. Comp. Fluid Mech.*, 8, 193-210. DOI: 10.1080/19942060.2014.11015507.